

REMARKS

Claims 16-23 are pending. Claim 21 stands withdrawn from further consideration as being directed to a non-elected species. Applicants propose amendment of claims 16 and 23.

Claims 16-20, 22 and 23 are rejected under 35 USC 103(a) as being unpatentable over Tsang in view of Fukagi. Favorable reconsideration of this rejection is earnestly solicited.

One of ordinary skill in the art would not have been motivated by the teachings of Fukagi to make the modifications of Tsang asserted by the Examiner due to the differences in the basic structures of each reference. The ridge of Tsang is selectively grown through a stripe opened in an oxide layer covering a cladding layer. On the other hand, the ridge structure of Fukagi is formed by etching, as illustrated in Fig. 20 and described at column 14, lines 47-67. Based on these different formation techniques, one of ordinary skill in the art would not have been motivated to modify Tsang as asserted by the Examiner.

In order to clearly distinguish the invention from the cited art, applicants propose amendment of claims 16 and 23 to specify an off-angle of 2 ° to 30 °. The cited references teach away from the claimed range. Each of Tsang and Fukagi is directed to a long wavelength lasers whereas the claimed invention is directed to a light-emitting device enabling shorter wavelength, low threshold and high temperature operation.

In the working example of Tsang, the InP cladding layer in the ridge structure is formed by liquid phase epitaxy (LPE). The detail of the growing condition is described in column 5,

lines 4-15. When a substrate having a larger off-angle is used in LPE, abnormal crystal growth locally occurs more frequently. It is stated in "Singular instabilities on LPE GaAs, CVD Si and MBE InP growth surfaces", D. L. Rode, W. R. Wagner and N. E. Schumaker, Appl. Phys. Lett. 30, 75 (1977) that when the crystallographical plane of the substrate used in LPE is not (100), the surface of the obtained crystal has a terraces-like pattern. A copy of this reference is attached. The reference concludes that off-angle of the substrate must be within plus-minus 0.1° to a crystallographic plane of (100). Thus, the reference teaches away from application of the substrate having an off-angle of 2° to 30° . No one skilled in the art would have been motivated to use substrate having an off-angle of 2° to 30° .

Fig. 4 of Tsang shows a DFB laser in which distributed feedback grating is formed. It is important for improvement of the function of DFB laser that the distributed feedback grating forms an ideal sine curve. However, when an off-angle substrate is used, DFB laser function becomes poor. This is because bilateral symmetry is lost due to off-angle and therefore a distributed feed back grating having a predetermined period can not be produced as designed. One skilled in the art accordingly would use a substrate having no off-angle in a DFB laser. In other words, no one skilled in the art would have been motivated to use the substrate having an off-angle of 2° to 30° .

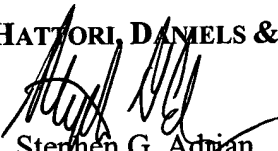
For at least the foregoing reasons, the claimed invention distinguishes over the cited art and defines patentable subject matter. Favorable reconsideration is earnestly solicited.

Amendment After Final Rejection
Serial No. 10/652,342
Attorney Docket No. 990342A

Should the Examiner deem that any further action by applicants would be desirable to place the application in condition for allowance, the Examiner is encouraged to telephone applicants' undersigned attorney.

If this paper is not timely filed, Applicants respectfully petition for an appropriate extension of time. The fees for such an extension or any other fees that may be due with respect to this paper may be charged to Deposit Account No. 50-2866.

Respectfully submitted,
WESTERMAN, HATTORI, DANIELS & ADRIAN, LLP


Stephen G. Adrian
Attorney for Applicants
Registration No. 32,878
Telephone: (202) 822-1100
Facsimile: (202) 822-1111

Attachment: Applied Phys. Lett. 30, 75 (1977)

SGA/arf

reasonable certainty that the first stage in the evolution of stacking faults is the formation of silicon-oxygen clusters as envisioned in the model.

In summary, a model for the formation of stacking faults in silicon is proposed, and the three envisioned stages are schematically illustrated in Fig. 1. Experimental evidence in support of the model has been developed by examining microstructural features in oxidized {100} Czochralski silicon wafers by transmission electron microscopy. Of particular importance in these samples is the absence of perfect dislocations, as noted in an earlier report.²⁵ Furthermore, based on the above model, the observed role of point-defect clusters constituting the swirl pattern in FZ crystals, precipitates in CZ crystals, grown-in abrasion-induced dislocations and the influence of the SiO₂/Si interface on the generation of stacking faults can satisfactorily be accounted for.

The authors would like to acknowledge fruitful discussions with G. Y. Chin and appreciate his comments on the manuscript.

¹D. J. D. Thomas, *Phys. Status Solidi* 3, 2261 (1963).

²H. J. Queisser and P. G. G. van Loon, *J. Appl. Phys.* 35, 3066 (1963).

³G. R. Booker and R. Stickler, *Philos. Mag.* 11, 1303 (1965).

⁴W. A. Fisher and J. A. Amick, *J. Electrochem. Soc.* 113, 1054 (1966).

⁵M. L. Joshi, *Acta Metall.* 14, 1157 (1966).

⁶J. E. Lawrence, *J. Appl. Phys.* 40, 360 (1969).

⁷S. Prussin, *J. Appl. Phys.* 43, 2850 (1972).

⁸C. M. Hsieh and D. M. Maher, *J. Appl. Phys.* 44, 1302 (1973).

⁹K. V. Ravi and C. J. Varker, *J. Appl. Phys.* 45, 263 (1974).

¹⁰W. K. Tice and T. C. Huang, *Appl. Phys. Lett.* 24, 157 (1974).

¹¹M. Conti, G. Corda, R. Matteucci, and C. Ghezzi, *J. Mater. Sci.* 10, 705 (1975).

¹²J. R. Patel and A. Authier, *J. Appl. Phys.* 46, 118 (1975).

¹³P. B. Hirsch, *NPL Conference on the Relation between Structure and Strength in Metals and Alloys* (Her Majesty's Stationary Office, London, 1962), p. 440.

¹⁴G. R. Booker and W. J. Tunstall, *Philos. Mag.* 13, 71 (1966).

¹⁵F. B. Pickering, in Ref. 13, p. 398.

¹⁶J. R. Patel, *Discuss. Faraday Soc.* 38, 201 (1964).

¹⁷D. Bialas and J. Hesse, *J. Mater. Sci.* 4, 779 (1969).

¹⁸R. W. K. Honeycombe, J. S. T. van Aswegen, and D. H. Warrington, in Ref. 13, p. 380.

¹⁹J. M. Silcock and W. J. Tunstall, *Philos. Mag.* 10, 361 (1964).

²⁰K. V. Ravi, *Metall. Trans.* 4, 681 (1973).

²¹I. R. Sanders and P. S. Dobson, *Philos. Mag.* 20, 881 (1969).

²²R. W. G. Wyckoff, *Z. Kristallogr.* 62, 189 (1925).

²³H. Foil and B. O. Kolbesen, *Appl. Phys.* 8, 319 (1975).

²⁴R. Stickler and G. R. Booker, *Philos. Mag.* 8, 859 (1963).

²⁵G. A. Rozgonyi, S. Mahajan, M. H. Read, and D. Brasen, *Appl. Phys. Lett.* 29, 531 (1976).

Singular instabilities on LPE GaAs, CVD Si, and MBE InP growth surfaces

D. L. Rode, W. R. Wagner, and N. E. Schumaker

Bell Laboratories, Murray Hill, New Jersey 07974

(Received 9 August 1976; in final form 18 October 1976)

Singular instabilities at crystal growth interfaces of group-IV and III-V semiconductors lead to as-grown surfaces which exhibit terraces and pyramids. Most electronic and optical devices, however, require the achievement of smooth planar layers. We consider the stability of surfaces with respect to singular instabilities and show that stable planar growth interfaces occur at slight deviations from the singular orientation where monatomic growth steps are uniformly arrayed to minimize the interfacial energy resulting from step-step attractive interactions. These results are applied to the elimination of crystal growth terraces in LPE AlGaAs-GaAs laser material. Similar considerations appear to explain pyramid formations on CVD Si and on MBE InP.

PACS numbers: 68.55.+b, 68.48.+f, 81.15.-z, 42.55.Px

A recent paper by Rode¹ shows how sub-angstrom displacements² of atoms at monatomic steps on crystalline surfaces can give rise to energetically attractive step-step interactions. These interactions were used to explain the orientation dependences³ of vapor-phase epitaxial (VPE) growth rates of GaAs on vicinal {100} surfaces. Since a sizeable interaction of this sort may, under certain circumstances, lead to a condensation of monatomic steps into macroscopic surface morphological features,¹ we report here appropriate interfacial stability conditions for crystalline growth surfaces and point out a number of experimental results gathered over the last two decades which appear explicable by these means.

Because several morphological features (such as terraces, pyramids, sides of plateaus, hillocks) evi-

dent during crystal growth take on relatively large lateral dimensions compared to monatomic step spacings^{1,5,6} (1–100 μm compared to 0.002–0.05 μm), we may simply consider the one-dimensional energetic stability of a solid surface near a low-index singular orientation stabilized by⁴ surface reconstruction. We take the specific energy of the singular surface to be γ_0 , while the generalized surface energy for nearby orientations, $\gamma(\varphi)$, depends in a calculable manner¹ upon the misorientation angle φ measured from the singular surface. If now the initial φ -oriented surface is permitted to decompose continuously, by rearrangement of the monatomic step spacings, into a micro-faceted surface containing only $\varphi=0$ singular treads and $\varphi=\theta$ nonsingular risers of macroscopic scale, we find by straightforward calculation that the overall

surface energy at constant *average* orientation will have been lowered if the following condition holds true:

$$(\gamma_0/\sin^2\varphi) + (\partial/\partial\varphi)[\gamma(\varphi)/\sin\varphi] < 0,$$

unstable with respect to singular features. (1)

That is to say, vicinal growing (or etching) interfaces are energetically unstable with respect to singular morphological features if the surface energy decreases sufficiently rapidly with orientation approaching the singular one. The stability criterion (1) is to be noted as distinct from the well-known expression not involving singular surfaces as developed earlier by Chernov,⁷ and Cabrera and Coleman.⁸ Indeed, there exists a number of functions $\gamma(\varphi)$ which predict *stability* under the one condition^{7,8} and *instability* under the present expression (1). Since singular features present demonstrably more stringent conditions for stability, we discuss below experimental examples for which (1) seems applicable as these cases appear readily obtainable in practice.

One of the most commonly observed, and technologically annoying, manifestations of singular instabilities during semiconductor crystal growth is the appearance of crystal growth terraces which occur in liquid-phase epitaxial (LPE) growth of very thin (0.1–0.3 μm) layers

of AlGaAs and GaAs for heterostructure lasers.^{5,9,10} [See Figs. 1(a) and 1(b)]. Such terraces also appear on VPE-grown GaAs¹ and on LPE-grown Si, Ge, GaP, GaSb, InP, and SiC.¹ A truly remarkable aspect of this type of morphology is that the riser orientation lies only 0.8–0.9 deg away from the singular tread orientation, in some cases,⁵ suggesting an atomic step spacing on the riser itself which is 180–200 Å while the monatomic step height is only 2.8 Å. This result suggests the long-range nature of the step interaction discussed by Rode.¹

By use of expression (1) and the surface energy formula derived earlier,¹ we find that a surface initially misoriented off the singular by the tread-to-riser angle θ should be stable with respect to singular terrace formation. It is worth emphasizing that, for given growth conditions, this particular θ orientation is uniquely stable—almost as though the surface were in tension for misorientations smaller than θ and in compression for misorientations greater than θ . Hence, we refer to these as *critically* oriented substrates as distinct from *misoriented* substrates ($\varphi \gtrsim 3$ deg) and *nominally* oriented substrates, e.g., $\{100\} \pm$ incipient cutting errors generally near 0.1 deg.

The results of growth on critically oriented substrates are shown in Figs. 1(c) and 1(d) where we show the essential absence of terraces in the as-grown surface [Fig. 1(c)] as well as in an underlying active layer of a heterostructure laser wafer [Fig. 1(d)]. The terraces shown in the active layer demonstrate that singular terraces are indeed present *during* crystal growth and are not developed due to termination of the growth process. We remark here also that, as might be expected from the relatively small number of nucleation sites at atomic steps, trace impurity and dopant concentrations readily affect the detailed structure of terraces. We have determined the critical angle θ for $\text{Al}_x\text{Ga}_{1-x}\text{As}$ with $0 \leq x \leq 0.36$ at growth temperatures from 730 to 880°C on nominal $\{100\}$ and $\{111\}$ As substrates and find that (a) θ tends to decrease with increasing x or temperature, probably due to thermal vibrations of atoms at steps; and (b) θ is ordinarily larger for $\{111\}$ As surfaces, indicating a more pronounced step interaction. Indeed, thermal vibrations smear out the criticality of θ to ± 0.1 deg so that above 350°C on $\{100\}$ where θ has decreased to below about 0.1 deg, the terrace instability is destroyed. On the other hand, terraces on nominal $\{111\}$ As surfaces are readily apparent above 880°C and perhaps continue to be so at much higher temperatures. Indeed, this persistence may explain the appearance of these surfaces as large singular facets on melt-grown GaAs crystals pulled from the melt at 1238°C.¹¹

Before closing our discussion, we point out two further examples of singular morphological features developed on chemical-vapor-deposited (CVD) Si crystals and on molecular-beam-epitaxial (MBE) InP crystals.

The CVD Si crystal shown in Fig. 2 was grown by the standard $\text{SiCl}_4\text{-H}_2$ process commonly used for integrated circuits materials.¹² Growth of the 4- μm -thick (average) epitaxial Si layer took place on the $\{111\}$ Si substrate for 3 min at 1130°C after initial growth at 900°C for 1 min. Large tripramids containing three major facets and three minor facets are readily apparent in

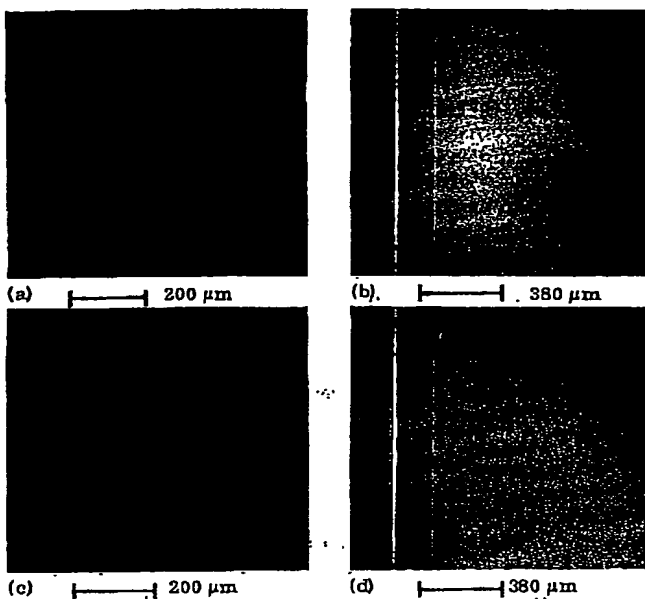


FIG. 1. Double-heterostructure GaAs-AlGaAs laser crystals LPE grown at 775°C on nominal $\{100\} \pm 0.1$ deg substrates [(a) and (b)] and on critically oriented substrates $\{100\} + 0.8 \pm 0.1$ deg, (c) and (d)]. Parts (a) and (c) show as-grown GaAs surfaces of four-layer heterostructures (Nomarski contrast) with and without terraces (Ref. 5). Parts (b) and (d) show photoluminescence responses from the 0.15- μm GaAs active layer (third below the surface) lying about 2 μm beneath the surface (Ref. 10). Note that terraces on the surface and in the GaAs active layer are suppressed in parts (c) and (d) by the critical orientation. Although the critical orientation for the underlying AlGaAs layer is different from that of the GaAs layer, the step interaction on AlGaAs is sufficiently weak to prevent substantial terracing under these conditions.

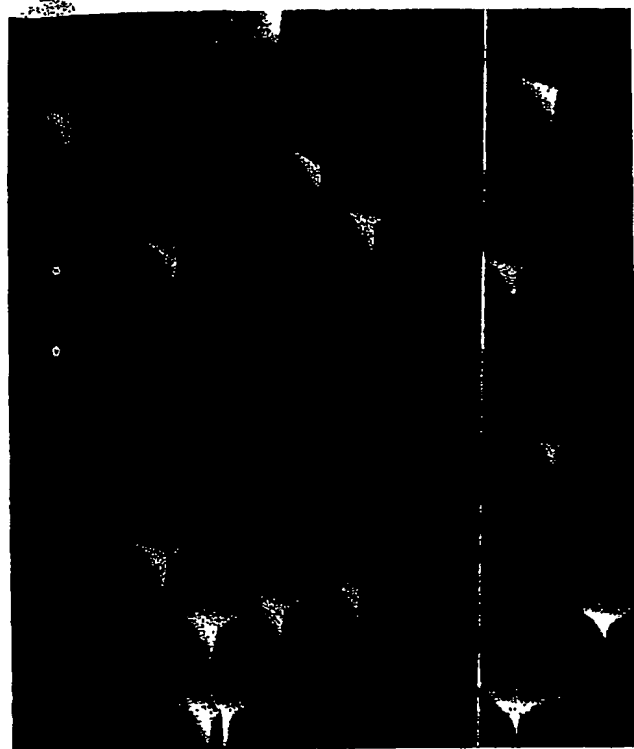


FIG. 2. Epitaxial CVD Si grown on (111) (Ref. 12) yields large tripyramids with three stable major facets lying 0.45 deg off (111) and three smaller unstable minor facets which are slightly bifurcated. The Nomarski contrast used for the photomicrograph yields constant hue for constant surface slope. Hence, the uniform hue along major facets indicates fixed atomic step spacings of about 400 Å. During growth, the steps propagate in the $[1\bar{1}2]$ and equivalent directions so that Si atoms at steps exhibit double dangling bonds. The "white caps" at some of the peaks are more steeply sloped (~ 1.2 deg) after growths apparently occurring during shut-down of the furnace and termination of growth. The critical angle increases with decreasing temperature.

Fig. 2.¹³ The relative instability of the three minor facets is evidenced by their irregular bifurcation shown in Fig. 2 and by their disappearance in favor of the major facets at lower growth temperatures (e.g., 980°C). The stable major facets appear to be formed due to the step interaction discussed above—these facets lie off (111) by only 0.45 deg so that atomic steps 3.1 Å high are uniformly arrayed with a spacing of 400 Å along the facet. This result again illustrates the remarkably long-ranged nature of the elastic step interaction.¹ Clearly, there is a strong in-plane anisotropy of step energy for Si as portrayed by the sharply angular nature of the tripyramids. The propagation direction of these steps during growth has been clearly determined by x-ray diffraction to be $[1\bar{1}2]$, i.e., steps with *two* unsaturated bonds per step atom, as opposed to the $[11\bar{2}]$ steps with *one* unsaturated bond per atom that might have been expected on simple grounds of the truncated lattice. This preference for $[1\bar{1}2]$ step direc-

tions on Si has been noted by Abbink, Broudy, and McCarthy¹⁴ for vacuum-deposited Si, by Henzler¹⁵ for high-vacuum annealed cleaved Si, and by the present authors on $\text{SiH}_4\text{-H}_2$ CVD Si prepared by Henderson and Helm.¹⁶ Thus, the appearance of steps with double unsaturated bonds (in the truncated-bond scheme) occurs under a variety of ambients for temperatures from room temperature to 1200°C. It is interesting that Schlüter *et al.*¹⁷ calculate energetically lowered surface states associated with $[1\bar{1}2]$ steps compared to $[11\bar{2}]$ steps, although the total step energy has not been calculated. In a related crystal, Tikhonova¹⁸ also reports observing $[1\bar{1}2]$ steps on MBE Ge, which leads us to results concerning MBE InP.

Miller and McFee¹⁹ have grown MBE InP on nominal (111) P substrates at 410°C. The substrate edges, however, are rounded slightly off (111) P by polishing so that rather straight terraces similar to those shown in Figs. 1(a) and 1(b) develop toward $[11\bar{2}]$ directions because of the slight misorientation. Nearer the substrate center oriented along (111) P, tripyramids very much like those on (111) Si,^{12,13} are found with stable facets which we have measured to lie only 0.88 deg off (111) P. Unlike Si, the steps are oriented so as to possess In atoms at $[11\bar{2}]$ steps with only one broken tetrahedral bond while the remaining three bonds to the P sublattice are intact. It seems a most natural circumstance for the steps on InP to orient themselves such that only one tetrahedral bond of the three-valent In atoms is uncoordinated while three survive intact.

In conclusion, we have shown for the case of LPE GaAs that one can obtain epitaxial growth interfaces which are stable with respect to singular instabilities by choosing critically oriented substrates. The present method relies on *energetic* stability of the interface so that considerable freedom in choosing low levels of impurity doping is maintained while near-equilibrium slow growth rates are permissible.

We are grateful to our colleagues at Bell Laboratories, M. Kowalchik, F. R. Nash, R. G. Sobers, and D. L. Van Haren, for providing technical support and unpublished experimental results. C. L. Paulnack and K. E. Benson provided the Si epitaxy reported here. J. H. McFee provided MBE InP material also reported here.

¹D. L. Rode, Phys. Status Solidi A 32, 425 (1975).

²Atomic displacements at steps are in the neighborhood of 0.3 Å (Ref. 1).

³L. Hollan and C. Schiller, J. Cryst. Growth 22, 175 (1974).

⁴J. C. Phillips, Surface Sci. 40, 459 (1973).

⁵D. L. Rode, J. Cryst. Growth 27, 313 (1974).

⁶M. Shimbo, J. Nishizawa, and T. Terasaki, J. Cryst. Growth 23, 267 (1974).

⁷A. A. Chernov, J. Cryst. Growth 24/25, 11 (1974).

⁸N. Cabrera and R. V. Coleman, in *The Art and Science of Growing Crystals*, edited by J. J. Gilman (Wiley, New York, 1963), p. 3.

⁹E. Bauser, M. Friik, K. S. Loechner, L. Schmidt, and R. Ulrich, J. Cryst. Growth 27, 148 (1974).

¹⁰F. R. Nash, R. W. Dixon, P. A. Barnes, and N. E. Schumaker, Appl. Phys. Lett. 27, 234 (1975).

¹¹C. Z. LeMay, J. Appl. Phys. 34, 439 (1963).

- ¹²The Si epitaxy was prepared by C.L. Paulnack and K.E. Benson of Bell Laboratories at Allentown, Penn.
¹³For similar results see the data presented by J.E. Allegretti, U.S. Patent No. 3,325,314 (1967).
¹⁴H.C. Abbink, R.M. Broudy, and G.P. McCarthy, J. Appl. Phys. 39, 4673 (1968).
¹⁵M. Henzler, Surf. Sci. 36, 109 (1973).

- ¹⁶R.C. Henderson and R.F. Helm, Surf. Sci. 30, 310 (1972).
¹⁷M. Schlüter, K.M. Ho, and M.L. Cohen, Phys. Rev. B 14, 550 (1976).
¹⁸A.A. Tikhonova, Kristallografiya 20, 615 (1975) [Sov. Phys. Cryst. 20, 375 (1975)].
¹⁹B.I. Müller and J.H. McFee, ECS Meeting, Extended Abstracts, 1976 (unpublished).

Acoustic pulse echo measurements at 200 MHz*

B. T. Khuri-Yakub and G. S. Kino

Edward L. Ginzton Laboratory, Stanford University, Stanford, California 94305
 (Received 12 July 1976; in final form 11 November 1976)

We have carried out acoustic pulse echo measurement with 2-nsec-wide pulses. These are used to excite a zinc oxide layer deposited on a conically shaped sapphire buffer rod 2 mm in diameter at the tip of the cone. We have found that an easy way to make contact between the sapphire rod and a solid material under study is by means of a gold foil. We have measured the thickness of a nickel plating on aluminum of the order of 50 μm , and that of a 134- μm -thick glass slide to within 2%.

PACS numbers: 43.85.+f, 81.70.+r, 06.60.Jn, 81.20.Lb

The basic aim of this work has been to extend acoustic pulse echo measurement techniques to frequencies of the order of 200–400 MHz. This involves using pulse lengths in acoustic media of the order of 20–50 μm . For this purpose we have employed transducers of a type originally developed for delay lines of rf-sputtered ZnO on a sapphire buffer rod.

The problems that we expected to encounter were as follows: (1) Excessive propagation loss in materials other than single crystals—experimentally this turned out to be reasonably low in ceramics such as Si_3N_4 , SiC, and MgO which we were interested in measuring. (2) Making a good acoustic contact with the ceramic—by using the self-aligning jig illustrated in Fig. 1, a small contact area and either gold foil or water between the sapphire rod and the ceramic, a low-loss contact could be made repeatedly, with a very small reflection coefficient between sapphire and materials with a similar acoustic impedance.

The transducer consists of an 8- μm -thick ZnO film rf sputtered on an (0001)-oriented sapphire rod with a 1000-Å-thick gold film in between as a backing for the transducer, and a 0.75-mm-diam 1000-Å-thick top dot as the exciting electrode; this defines the size of the acoustic beam. This beam diameter was chosen as the minimum to obtain negligible diffraction spreading at 200 MHz in a Si_3N_4 sapphire sample 1 cm long. As shown in Fig. 1, the sapphire buffer rod is in the form of a cone 5 mm long and 2 mm in diameter at the small end; the diameter of the small end is chosen so as to be able to make easy contact to flat materials without the application of excessive pressure and to be considerably larger than the beam size. The center frequency is 200 MHz, and the measured bandwidth is of the order of 200 MHz. We consistently obtain a coupling coefficient of at least 90% of the theoretical value $K_t = 0.28$.¹

We have constructed an avalanche transistor pulser circuit to generate 2–5-nsec 15–100-V rf pulses. A protection circuit, using Schottky diodes in a manner similar to that employed at lower frequencies, was used to protect the receiver section of the apparatus from the large transmitter pulse. Reflected pulses below 0.5 V pass through the protective circuit with very little change in amplitude and pulse shape. The signals were amplified with a broadband amplifier and measured on a 500-MHz oscilloscope.

We have used both water and a 1-mil-thick gold foil to make contact between the sapphire buffer rod and ceramics and other materials. Both techniques have yielded good results. However, we have used the gold

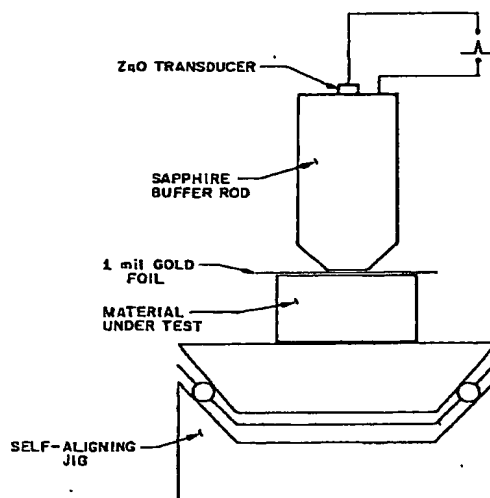


FIG. 1. A schematic of the fixture used for pulse measurements.